JOURNAL OF SOLID STATE CHEMISTRY 88, 207–216 (1990)

Magnetic Pairing of Charge Carriers in Doped Mott Insulators

N. KUMAR

Department of Physics, Indian Institute of Science, and Jawaharalal Nehru Centre for Advanced Scientific Research, Bangalore 560 012, India

Received March 6, 1990

DEDICATED TO J. M. HONIG ON THE OCCASION OF HIS 65TH BIRTHDAY

1. Introduction

The recent discovery (*1, 2*) of superconductivity in certain CuO_2-based layered perovskites with transition temperatures ($T_c \sim$ 30–125 K) spanning the boiling point of liquid nitrogen (77 K) has been one of the greatest surprises of the physics and chemistry of the transition metal oxides. Notable examples are the "214" compound $La_{2-x}(Ba, Sr)_x CuO_4$ ($T_c \sim$ 30–40 K, $x \sim 0.15$) (*2–4*), the "123" compound $YBa_2Cu_3O_{7-\delta}$ ($T_c \simeq$ 90 K, $\delta \simeq 0$) (*5*), and the family of Bi- and Tl-based compounds (Bi–Sr–Ca–Cu–O ($T_c \sim$ 110–120 K) (*6*) and Tl–Ba–Ca–Cu–O ($T_c \sim$ 118–140 K) (*7*) with variable numbers of CuO–CaO layers per chemical unit cell. These are highly "chemical" superconductors and can be tuned stoichiometrically to one's advantage over a rather wide range of stability limits. There are now compelling reasons to believe that the possibly unconventional (non-BCS) superconductivity, the high transition temperatures, and almost certainly the highly anomalous normal-state properties (*9*) of these layered oxides derive essentially from the strong electron–electron repulsion (correlation) and the low dimensionality ($D = 2$) found in these systems (*10*). In fact, these systems are best viewed as doped Mott insulators in the proximity of the (antiferromagnetic) insulator to (paramagnetic) metal transition (*11–13*). The latter has been studied extensively over the past 40 years or so in the context of transition metal oxides, and Professor Honig has made lasting contributions to our understanding of them. It is a pleasure to write for this *Festschrift* marking his 65th birthday.

This is not a review, however. What is presented here is a very specific (magnetic) mechanism for singlet pairing of charge carriers doped into the Mott insulators. The mechanism involves an intrinsically strong interaction of the charge carriers with the spin configurations of the antiferromagnetically (AF) correlated background. The idea is basically simple and can be readily visualized by reference to Fig. 4 that shows a mobile vacancy moving in an AF background assumed Néel-like, for simplicity. The moving vacancy lays down a "string" of overturned spins, the string tension being twice the exchange coupling J. A second vacancy can now "hoover" up the "string" and the pair can comove freely gaining thus the energy of delocalization. This argument that works well for the Ising case can be generalized for the case of Heisenberg AF on the basis of a time-scale argument to be introduced later. The idea of such a "string" is not new. It was used earlier to discuss the

0022-4596/90 $3.00

possible autolocalization of charge carriers in AF semiconductors (*14*). Following the discovery of high-T_c superconductivity, the idea was revived independently and almost simultaneously by several workers, within the framework of the two-band (*15, 16*) and the single-band (*17–19*) Hubbard model.

It seems apt at this stage to motivate this search for a non-phonon mechanism of pairing. But first let us note that the idea of pairing (which is central to BCS) itself is not in doubt. Observation of flux quantum and quantized vortices in units of $hc/2e$, of Shapiro voltage steps of spacing $\nu h/2e$, and of ac Josephson radiation at frequency $\nu = 2eV/h$ all verify $2e$ and not e as the charge on the supercurrent carriers. There are, however, strong reasons to discount phonons as mediating the pairing. The smallness of the otherwise expected oxygen isotope effect in the "214" compounds and its total absence in the 123 compounds argue against it. But the most convincing reason follows from its incompatibility with the normal-state resistivity which is linear in temperature from T_c right up to ~1000 K and beyond without any sign of saturation (*9, 20*). Writing $\rho(T) = 4\pi/\omega_p^2\tau$, with ω_p as the plasma frequency known from penetration depth and $1/\tau = 2\pi\lambda k_B T/\hbar$, where λ is the dimensionless electron–phonon interaction strength, it turns out that the linear resistivity-compatible value of λ is too low ($\lambda \lesssim 1$) to account for high $T_c \sim 90$ K. In the present magnetic pairing mechanism, however, the interaction-energy scale is set by the spin–spin exchange $J \sim 0.1$ eV which is sufficiently high. Of course, we are naturally limited to the Cuprate superconductors, and thus $BaPb_xBi_{1-x}O_3$ and $Ba_{1-x}K_xBiO_{3-\delta}$ are excluded from our discussion.

In order to make our discussion reasonably self-contained, let us recall some relevant experimental facts and generally valid theoretical considerations. For details reference may be made to the several review articles and conference proceedings now

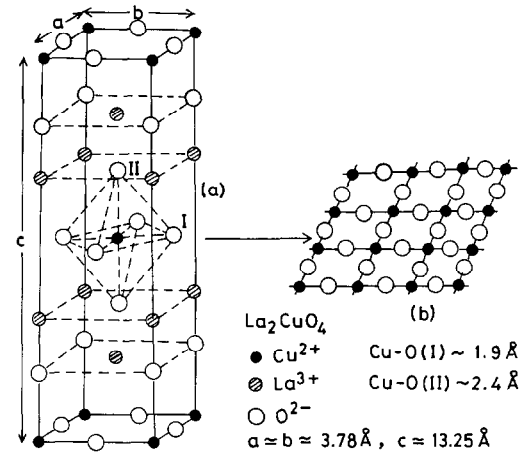

FIG. 1. (a) Crystal structure of La_2CuO_4; (b) CuO_2 plane.

available (*9, 21–27*). Consider the prototypical system $La_{2-x}Sr_xCuO_4$ whose crystal structure and phase diagram (*28*) are shown schematically in Figs. 1 and 2, respectively. The essential structural feature is the CuO_2 planes, separated by a relatively large distance of ~6 Å and, therefore, weakly coupled, making the system essentially two-dimensional electronically. This is supported by the observed large anisotropy of the resistive ($\rho_{ab}/\rho_c \sim 10^{-2}$), the magnetic ($J_{ab}/J_c \sim 10^5$), and the superconductive ($\lambda_{ab}/\lambda_c \sim 10$, λ penetration depth) properties. Resistive anisotropy as high as 10^5 is reported

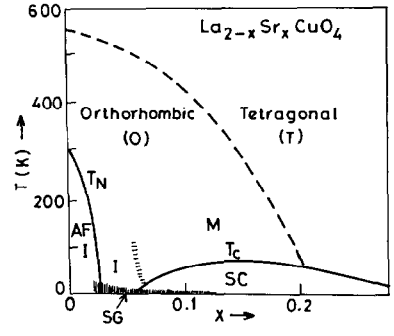

FIG. 2. Phase diagram of $La_{2-x}Sr_xCuO_4$ (schematic).

in some Bi and Tl compounds. The parent material La_2CuO_4 is confirmed by neutron diffraction to be an antiferromagnetic insulator with the Néel temperature $T_N \simeq 300$ K. The saturation magnetic moment residing on copper is ~0.6 μB which is less than the full Cu^{2+} value of 1.1 μB due to the 2D zero-point spin fluctuations. The remarkable feature of the phase diagram is the rapid degradation of T_N with doping. Thus $T_N = 0$ for $x > 0.02 \ll$ the site percolation threshold = 0.41 for a 2D square lattice. Thus the loss of long-range order (LRO) is not naively percolative as observed in the magnetically diluted systems, e.g., $Rb_2Mn_{1-x}Mg_xF_4$ or $Rb_2Co_{1-x}Mg_xF_4$ having the same K_2NiF_4 structure as La_2CuO_4. Moreover, the paramagnetic region of the AF regime ($T > T_N$) is also insulating! This implies that the system is a localized, Mott–Hubbard insulator rather than an itinerant, commensurate spin-density wave (SDW) insulator (*12*). For the latter, antiferromagnetism and insulation should coterminate at T_N. Indeed, the observed conductivity gap ~1–2 eV is far greater than what one would expect for an SDW, namely ~0.1 eV. As we traverse the doping (x) axis, the system becomes metallic (and superconductive at low temperatures) for $x > 0.05$. The T_c reaches a maximum at about $x \simeq 0.15$. The narrow region $0.02 < x < 0.05$ is semimetallic with variable range-hopping conductivity and, presumably, is a spin–glass (SG) at low temperatures, with randomly frozen spin directions. Neutron scattering (*28*) yields a dynamic structure factor for the insulating regime which is in excellent agreement with that calculated (*29*) for a 2D Heisenberg spin 1/2 system with $J_{11} \sim 0.1$ eV. The structure factor is completely dynamic for $T > T_N$ with long in-plane correlation length. On lowering the temperature through T_N, three-dimensional ordering is induced by the weak interplanar coupling $J_\perp \sim 10^{-5} J_{11}$ when the 2D correlation length becomes sufficiently large, ~1000 Å. The in-plane correlation length

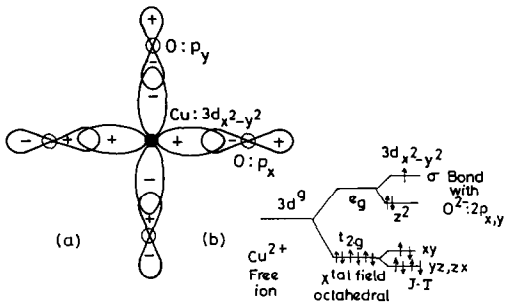

FIG. 3. (a) Cu^{2+}: $3d_{x^2-y^2}$ hybridization with O^{2-}:$2p_{x,y}$ in the CuO_2 plane; (b) Crystal field splitting (schematic).

diminishes rapidly with doping and in the metallic regime it is of the order of the mean intercarrier spacing. Perhaps, the single most important finding is that the copper moments retain their full value even in the metallic regime (*28*). Thus, the paramagnetic metallic regime is only apparently Pauli-like. The carriers move through a complex localized-spin background having short-range correlation, ~10 Å. The time-averaged moment is, of course, zero. This picture of spatially correlated moments both in the insulating paramagnetic as well as the metallic region with zero time average is consistent with the observed EPR silence (*30*). Further, the destruction of superconductivity for less than 5 at. % Zn substitution (*31*) for Cu implicates the copper spins in the mechanism for superconductivity.

We will end this Introduction with a brief discussion of the crystal quantum chemistry that should lead us to a minimum model to work with. Known valence states of lanthanum (La^{3+}) and oxygen (O^{2-}) in oxides force copper to be divalent (Cu^{2+}) for charge neutrality. Now, the Cu^{2+} ion is in the $3d^9$ configuration with five-fold orbital degeneracy. The crystal field of CuO_6-octahedron (Fig. 1a), however, splits the level into a threefold degenerate t_{2g} level (occupied fully) and a twofold degenerate e_g level (partially occupied) as shown schematically in Fig. 3b. Now, the CuO_6 octahedron is actu-

ally elongated with the copper-apical oxygen O(II) distance 2.4 Å while the Cu–O(I) distance in the basal plane is 1.9 Å. This Jahn–Teller (JT)-like distortion splits the e_g level further into an upper-half filled level $3d_{x^2-y^2}$ and a lower completely filled level $3d_{z^2}$. This is a purely ionic limit. The right symmetry of the directed Cu: $3d_{x^2-y^2}$ orbital and the $0:2\,p_x$, $2p_y$ orbitals of the ligands in the basal plane result in their strong hybridization. This leads to a lowest lying bonding band (full), a highest antibonding band (half-filled), and the remaining are nonbonding intermediate-energy bands (full). Thus, band theory predicts La_2CuO_4 to be a metal, contrary to the known facts. What is missing here is the electron–electron repulsion (correlation) which is large for the relatively localized $3d$ orbitals of copper. This disfavors the $3d^9 + 3d^9 \rightarrow 3d^8 + 3d^{10}$ transfer process involving energy cost (U) of double occupancy. Thus, for $U >$ the gain in energy by delocalization ($\simeq$ half the band width), the system must be an insulator—an odd electron Mott–Hubbard insulator (*12*). The observed AF coupling between the localized copper spins now arises through the superexchange via the bridging O^{2-} involving, for example, a virtual excursion of the two electrons on O^{2-} to the neighboring Cu^{2+} ions. This virtual process is blocked when the spins of the two Cu^{2+} ions, bridged by the O^{2-}, are parallel. We now consider doping, i.e., replacing the trivalent La^{3+}, by the divalent Sr^{2+}. The question now is where will the added "holes" be. It is convenient at this point to introduce the hole representation and take $|3d^{10}, 2p^6\rangle$ as the hole vacuum. Then Cu^{2+} will correspond to one preexisting hole on copper with the single-hole energy E_d, while O^- will correspond to an added hole on oxygen with energy E_p with $\Delta \equiv E_p - E_d$ as the charge transfer energy. Finally, Cu^{3+} will correspond to double hole occupancy with energy $2E_p + U$. It is clear that the added hole will create O^- or Cu^{3+} according to $\Delta < U$ or $\Delta > U$. Now, the spectroscopic data rules out Cu^{3+}: added holes are found to be on the oxygens (*32*). Hybridization will, of course, cause some charge transfer.

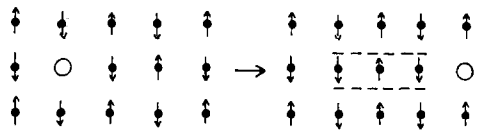

FIG. 4. Magnetic string (dashed line) due to hole (O) motion in Néel background.

These considerations motivate the following two-band Hubbard model (*16*) (in obvious notation)

$$\begin{aligned} \text{H (two-band)} = &\sum_{i,\sigma} \varepsilon_d d^+_{i\sigma} d^+_{i\sigma} + \sum_{l,\sigma} \varepsilon_p p^+_{l\sigma} p_{l\sigma} \\ &+ U \sum_i d^+_{i\uparrow} d_{i\uparrow} d^+_{i\downarrow} d_{i\downarrow} \\ &+ \sum_{i,\sigma,l} (V_{il} d^+_{i\sigma} p_{l\sigma} + h \cdot c). \end{aligned}$$

It turns out, however, that this model Hamiltonian is reducible to an effectively one-band Hamiltonian for strong hybridization. Here the added hole, spread coherently over the four ligands, forms a spin-singlet with the central copper hole gaining a considerable amount of hybridization energy. This singlet can now move as a quantum vacancy ("hole") in an effectively one-band Hubbard model (*33*). It is to be emphasized, however, that this is a composite object and acts as a structureless "hole" only for the low-energy phenomena.

The essential feature of the two-band model discussed above is that the two bands are *interlaced,* i.e., the oxygen hole moves via the intermediate $Cu^{1+}: 3d^{10}$ state involving spin-flip as shown schematically in Fig. 5 (it is possible for the oxygen hole to itinerate without (*34*) a spin-flip, but then the energetic advantage of hybridization is lost). We would like to call this "interlaced" band model a "*pdp*" model. This is to be contrasted with the "*pd*" model where the oxygen hole can hop directly to the neighboring

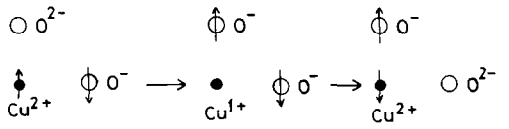

FIG. 5. Magnetic string (two interlaced bands). Oxygen hole (O^-) moves via copper Cu^{1+} state with spin-flip.

oxygen through a nonzero matrix element, and is merely exchange coupled to the copper hole. There is no "string" in this case. The one-band model is then the "*dd*" model where the hole moves as shown in Fig. 4. Any direct oxygen–oxygen matrix element will short-circuit the "string" mechanism and will be detrimental. It is our thesis that the interlacing discussed above and the associated coupling between the translational and the spin dynamics is the efficient cause of the unusual non-fermi-liquid behavior in the metallic normal state. It seems apt, therefore, to approach the metallic state from the insulating limit.

2. Model

I begin with the simplest Hamiltonian incorporating the strong on-site electron–electron correlation (repulsion), namely, the one-band Hubbard Hamiltonian in two dimensions given by (in obvious notation) (*35*)

$$H = -t \sum_{(i,j),\sigma} c^+_{i\sigma} c_{j\sigma} + h.c. + U \sum_i n_{i\uparrow} n_{i\downarrow} \qquad (1)$$

for n electrons on N lattice sites, and with $\delta \equiv 1 - n/N \equiv$ the deviation from half filling of the band. In the limit of strong coupling ($t/U \ll 1$) this can be transformed in the well-known spin-hole Hamiltonian (*35*),

$$\tilde{H} = -t \sum_{(i,j),\sigma} (1 - n_{i-\sigma}) c^+_{i\sigma} c_{j\sigma} (1 - n_{j-\sigma}) + h.c. + J \sum_{(i,j)} \left(S_i \cdot S_j - \frac{n_i n_j}{4} \right) + \cdots \qquad (2)$$

with $J = \dfrac{4t^2}{U}$,

operating in the subspace of nondoubly occupied sites. This is essentially the t–J model.

At exactly half filling ($\delta = 0$), $\tilde{H}$ is expected to describe a Mott–Hubbard insulator with antiferromagnetically correlated ground state in the thermodynamic limit (*12, 28, 29*).

We assume in the following that the AF correlation length is at least of the order of a certain microscopic length scale to be introduced and justified later. We now consider the quantum motion of a hole added at the origin. This, of course, is an intractable many-body problem. We now introduce a set of physically motivated approximations that reduce it to an effectively one-body problem which is exactly solved.

First, we note that the hole motion is locally fast while the spin fluctuations are relatively slow (*15, 17–19*). More precisely, the characteristic time scale of hole motion is $\tau_h \sim \hbar/t \ll \hbar/J \sim \tau_s$, the time scale of AF spin fluctuations due to exchange in the strong coupling limit. This suggests a quasistatic approximation (QSA) in which the AF spin background is locally replaced by a Néel-like static configuration so that the only spin dynamics is that concomitant with the hole motion relocating a spin, i.e., the spin dynamics is "slave" to the hole dynamics. Clearly, the QSA based on this time scale argument neglects the static spin distortion and zero-point spin fluctuations around the hole as well as the dynamic spin polaronic effect. We are still left with a nontrivial many-body problem in that the spin-hole configuration is not completely specified by the hole location alone. A closed-loop circuit by a hole does not in general return the system to the initial state. Inasmuch as the closed-loop motion is a higher order process and in any case involves entropic barrier, we introduce the retraceable path approxi-

mation (RPA), known to be reasonable for the local phenomena (*36, 37*). This effectively replaces the 2D lattice by a Bethe lattice of connectivity $K(=3$ in the present case). Now the state of the system is completely specified by the location of the hole. The Hilbert space consists of all states connected transitively by the hopping term in Eq. (2) to the origin where the hole was injected. The origin can, of course, be anywhere and in this sense the translational invariance is retained. With QSA and RPA the hole moves under the confining local potential $V_1(j) = jJ + \frac{3}{2}J$ due to the "string" of overturned spins, where the string tension $J = 4t^2/U$ corresponds to two broken lateral bonds and j is a length of the string in units of lattice spacing a, i.e., the self-avoiding walk (SAW) distance from the origin. We now study this one-body problem first.

3. One-Hole Case

The resulting one-hole Hamiltonian is now

$$H_h = -t \sum_{\langle i,j \rangle} (|i\rangle\langle j| + |j\rangle\langle i|) + \sum_j V_1(j)|j\rangle\langle j|. \tag{3}$$

We look for the ground state that must be a nodeless s-state. For the Bethe lattice the latter implies that the wave amplitude Φ_j depends only on $|j| \equiv j$. The eigenvalue equation is

$$-t\Phi_{j-1} - K\Phi_{j+1} + V_1(j)\Phi_j = E\Phi_j, j = 1, 2, \ldots \tag{4a}$$

along with the boundary condition

$$-t(K+1)\Phi_1 = \Phi_0. \tag{4b}$$

This is exactly reducible to quadrature for the eigenvalue E. For simplicity, however, we shall treat Eq. (4) in the continuum limit by setting $n \to x/a$, $\Phi_j \to \Phi(x)$ and expanding the differences up to second order in a. We get

$$1/2\,(K+1)a^2t\frac{d^2\Phi}{dx^2} + (K-1)at\frac{d\Phi}{dx} + \left(E - \frac{Jx}{a} + (K+1)t - 1.5J\right)\Phi = 0 \tag{5}$$

$$\text{with } \left(\frac{d\Phi}{dx}\right)_{x=0} = 0.$$

We check later that the continuum approximation is indeed reasonable.

The unnormalized eigenfunction is

$$\Phi(x) = e^{-\left(\frac{k-1}{k+1}\right)\frac{x}{a}} A_i(y) \tag{6}$$

$$\text{with } y = \frac{-\frac{2E}{(K+1)t} + \frac{2J}{(K+1)t}\frac{x}{a} + \left(\frac{K-1}{K+1}\right)^2 - 2 + \frac{3}{(K+1)}\frac{J}{t}}{\left(\frac{2J}{(K+1)t}\right)^{2/3}}.$$

Here $A_i(y)$ is the Airy function. The eigenvalue E is now determined by the boundary condition

$$\left(\frac{d \ln A_i(y)}{dy}\right)_{x=0} = \left(\frac{K-1}{K+1}\right)\left(\frac{(K+1)t}{2J}\right)^{1/3}. \tag{7}$$

In Fig. 6 we have plotted the single-hole

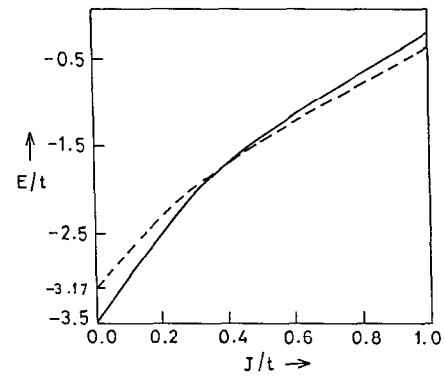

FIG. 6. J/t dependence of ground state energy of a single hole in t–J model. Solid line for hole confined by string of tension J (present work). Dashed line from numerical work of Dagotto *et al.* (*38, 39*) on 4 × 4 spin lattice.

ground state energy E^{1h} as function of J/t along with the numerical results of Dagotto *et al.* (*38, 39*). The agreement seems reasonable. As a check on the continuum approximation, we verify that for a discrete Bethe lattice the bottom of the "free band" is at $-2\sqrt{Kt} \simeq -3.46t$, not very far from its value $\simeq -3.5t$ obtained in our continuum limit. The spatial spread of the ground state is found from Eq. (6). Recalling that the Airy function for positive argument decays exponentially, the localization length for the ground state turns out to be $l_0 \simeq a((1 + K)U/t)^{1/3} \simeq 2$ to 4 lattice spacings. Thus the assumption that l_0 is at least of the order of the AF correlation length may not be unphysical. We emphasize once more that this autolocalization is strictly true only in the quasistatic limit $J/t \ll 1$ but outside of the Nagaoka well limit (*40*). For a t–J model in the opposite limit, i.e., $J/t \gg 1$, obviously the spins can follow the relatively slow hole motion adiabatically. There is no confining "string" and hence no localization. Instead, one has an essentially coherent band motion of the hole. In this limit the minimum hole energy measured from the bottom of the "free band" will scale linearly with J. Thus there exists an intermediate crossover ratio J/t where the autolocalization breaks down. This happens when the localized level-spacing (that can be shown from Eq. (7) to scale sublinearly with J) becomes less than J, the spin-flip matrix element. However, even in the quasistatic limit $J/t \ll 1$, the hole will delocalize on the *long time* scale due to the finite transverse (flip–flop) part of the exchange interaction. This will impart a resonant width $\simeq J \times$ overlap factor $\ll J$ to the otherwise sharp localized level.

4. Hole Pairing

Next we solve the same problem for two holes with the attractive "string" potential now $V_2(j) = jJ + J$, where j is the SAW distance between the holes in units of a. The topology of the Bethe lattice, representing effectively our RPA to the real 2D lattice, however, introduces a steric coupling between the center-of-mass (cm) motion and the relative motion. This complexity is simplified if we note that cm motion is free on the Bethe lattice with an effective transfer matrix element $t/2$ (mass doubling) while the relative motion corresponds to $2t$ (reduced mass) but is essentially with $K = 1$. That is to say that the relative motion stays parallel to the cm motion. The boundary condition for the relative wave function is that it must vanish for zero-separation—the holes have a hard core by definition. With this the calculated two-hole ground energy E_0^{2h} is plotted as function of J/t in Fig. 7. Clearly, the holes bind for $J/t > 0.45$.

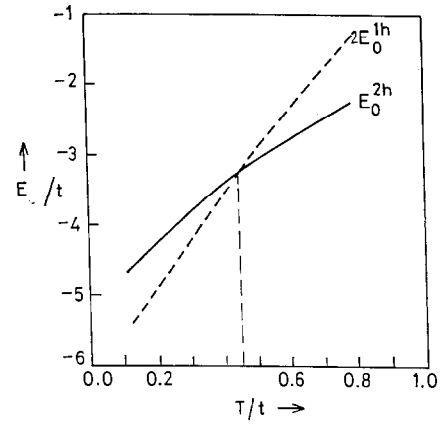

FIG. 7. Ground state energy E_0^{2h} of string-confined two-hole state (solid line). Twice the ground state energy E_0^{1h} of isolated holes (dashed line). Holes bind for $J/t > 0.45$.

5. Finite Concentration

We now study the effect of finite (but still small) hole concentration δ. We find two distinct effects, namely, the destruction of long-range AF order for $\delta > \delta_1 \simeq 0.025$ and the delocalization of holes by pairing for a somewhat higher concentration $\delta = \delta_2 \simeq$

0.04. The argument is as follows. The number of sites spanned by the localized hole wave function is $\simeq (l_0/a)^2$. The crucial point now is that the spins on these sites are dynamically compensated in the sense that the single-site susceptibility is drastically reduced to a value corresponding to a spin temperature $\simeq t/k_B \gg T$, the actual temperature. This can be understood semiclassically as a result of rapid reorientation of the spin at a given site due to the hole motion. This is confirmed by the exact calculation on a simple three-site problem (simulating, indeed, the original CuO_2 cluster where the O-hole moves from oxygen 1 to oxygen 2 mediated by Cu^{1+} involving the intermediate (Cu spin-flip) that gives the Cu site susceptibility to be $\sim g^2 \mu_B{}^2/4t$ which corresponds to a spin temperature $\sim t/k_B$. Thus, at a hole concentration δ, the fraction of spins magnetically "dead" is $\delta(l_0/a)^2$, the effective site dilution of the background AF. We expect the long-range order to be destroyed percolatively for $1 - \delta(l_0/a)^2 \leq p_c$ 0.59 giving $\delta_1 \simeq 0.025$ for our case, close to the observed value. The p_c is the site percolation threshold in $D = 2$. For higher concentrations, a new effect begins to operate, namely, that the unperturbed localized hole wave functions begin to physically overlap. Inasmuch as the holes have a hard core by definition, this excluded-volume effect must renormalize the localized single hole energy upward and thus favor the delocalized hole pairs energetically. This effect is expected to set in at a hole concentration $\delta = \delta_2 > \delta_1$ when the "volume fraction" occupied by the randomly centered hole-wave functions approaches the percolation threshold, that is for $\delta_2(l_0/a)^2 = p_c = 0.59$. (Note that δ_1 defined earlier corresponds to the complementary percolation threshold when the magnetically active sites just percolate). Thus $\delta_2/\delta_1 = p_c/(l - p_c) \simeq 1.5$ giving $\delta_2 \simeq 0.04$. Thus for $\delta > \delta_2$ we expect the localized hole-wave functions to physically overlap sufficiently such that the single-hole energy may be raised enough so as to favor compact pairs energetically. Superconductivity is now visualized as essentially due to Bose condensation of these pairs. The rise of T_c and its eventual fall with δ then follows (*41*) the behavior of lattice-bound Bose gas with hard core which is generally consistent with the known phase diagram. It is important to point out here that the present "string" mechanism of pairing cannot lead to clumping of holes (phase separation), for the "string"-mediated interaction saturates inasmuch as the "string" connects just two holes at its ends.

6. Discussion

The above hole localization and its delocalization by pairing has interesting implications for the normal state transport and optical absorption. The first excited 1-hole state has an energy $E_1^{1h} \simeq -1.3t$ found by imposing the boundary condition $\Phi(x = 0) = 0$ in Eq. (7). The excitation energy $E_1^{1h} - E_0^{1h} \simeq 0.5t$ is about 0.5 eV for $t \simeq 1$ eV, and should appear as an electronic peak in optical absorption spectrum. The peak should disappear with delocalization-by-pairing at higher hole concentration. (One should note that any intrapair excitation is not electric-dipole allowed due to the homopolar nature of the compact hole pairs). This feature should be looked for. As for the electrical transport, at low hole concentration $\delta < \delta_1$, the system is an AF insulator with long-range order. For $\delta_1 < \delta < \delta_2$, the long-range order is lost and the system is a nonmetal (semiconductor) with possibly variable-range hopping of localized holes. For $\delta > \delta_2$, however, delocalized by incipient hole-pairs should give even for $J/t < 0.45$ a diffusive conduction. The diffusion of the hole is determined by the favourable spin-flips caused by another hole passing adjacently, leading to a temperature-independent diffusion coefficient. This, together with the Einstein relation for a nondegenerate gas of holes, gives resis-

tivity linear in temperature. At low temperatures, the same pairs condense to give superconductivity. Thus $\delta = \delta_2$ marks not only the onset of superconductivity along the δ axis in the phase diagram but also a crossover from an insulating to a metallic regime in the normal state. These two features, namely that the insulating AF phase ends at $\delta = \delta_1 \simeq 0.025$ but the onset of superconductivity is delayed until $\delta = \delta_2 \simeq 0.04$ at $T = 0$ K, and that δ_2 also marks the insulator–metal crossover, are common to the phase diagrams reported for the high-T_c superconductors. We should note here that hole-pairing within a two-band Hubbard model has been demonstrated numerically by Hirsch *et al.* (*42*). As noted earlier in the Introduction, this is already expected because of its reducibility to a one-band Hubbard Hamiltonian for the low-energy phenomena (*43*).

Recently, the unusual metallic state has been attributed to a marginal Fermi-liquid behavior on phenomenological grounds (*44*). More specifically the linear in-plane resistivity $\rho_{ab}(T)\ \alpha\ T$ at low temperature, implying the carrier lifetime $\tau\alpha\ 1/T$, clearly violates the Fermi-liquid condition $\tau \gg \hbar/k_B T$. It is our belief that this short lifetime results from "dephasing by orthogonality" inherent to our present picture, namely that the partial amplitudes for the propagation of the "hole" via alternative paths add incoherently because the background spins are left in the mutually orthogonal states, in the quasistatic approximation ($J/t \ll 1$). This does not involve energy transfer. Such a complete incoherence has been pointed out earlier by Brinkman and Rice (*36*) in the atomic limit ($t/U \to 0$). For not a very small value of J/t, one may expect a coherent motion of the almost autolocalized hole with a resonance band width proportional to J times the spin-overlap factor, as for a polaron. For a finite concentration of holes, however, incoherence will result when the hole traverses a distance $\gtrsim$ mean carrier spacing during the typical spin fluctuation time $\sim\hbar/J$. This gives $\delta \gtrsim (\pi/8)^{3/2}(J/t)$ which for $t/U = 0.1$ gives $\gtrsim 0.07$. This amounts to holes interacting with highly damped (sloppy) spinwaves. Here we have assumed the holes to be spinless fermions moving with a Fermi speed corresponding to the hole concentration δ per site.

Finally, there is the disturbing question; namely, why does replacement of Cu^{2+} (spin 1/2) by Ni^{2+} (spin 1) destroy superconductivity. One suspects that the strong Hund's Rule intraatomic coupling makes the present mechanism energetically disfavored. Obviously, this calls for further study.

We conclude this discussion by saying that the motion of a "hole" (mobile vacancy) in the one-band model and the associated "string" are the very kernel of the problem of proper understanding of the normal and the superconducting states of these remarkable oxides.

Acknowledgment

The author thanks Professor C. N. R. Rao and the colleagues in the Condensed Matter Theory Group of the Department of Physics at this Institute for many an enlightening discussion.

References

1. J. G. Bednorz and K. A. Müller, *Rev. Mod. Phys.* **60,** 585 (1988).
2. J. G. Bednorz and K. A. Müller, *Z. Phys. B* **64,** 189 (1986).
3. S. Uchida *et al., Japan. J. Appl. Phys.* **26,** L1 (1987); C. W. Chu *et al., Phys. Rev. Lett.* **58,** 403 (1987).
4. J. M. Tarascon, *Science* **235,** 1373 (1987); R. B. Van Dover *et al., Phys. Rev. B* **35,** 5337 (1987).
5. M. K. Wu *et al., Phys. Rev. Lett.* **58,** 908 (1987); J. M. Tarascon *et al., Phys. Rev. B* **35,** 7115 (1987).
6. H. Maeda *et al., Japan. J. Appl. Phys.* **27,** L209 (1988).
7. Z. Z. Sheng and A. M. Hermann, *Nature (London)* **332,** 55 (1988).
8. A. M. Hermann *et al., Phys. Rev. B* **37,** 9742 (1988).
9. P. B. Allen *et al.*, "Physical Properties of High

Temperature Superconductivity" (D. M. Ginsberg, Ed.), Vol. 1, p. 213, World Scientific, Singapore (1989).
10. P. W. ANDERSON, "Proc. of the Enrico Fermi International School of Physics; Frontiers and Borderlines in Many-body Physics," North-Holland, Varenna (1987).
11. J. M. HONIG AND L. L. VANZANDT, *in* "Annual Rev. Mater. Sci." (R. A. Huggins, R. N. Bube, and R. W. Roberts, Eds.), Annual Review, Palo Alto (1975).
12. N. F. MOTT, "Metal Insulator Transition," Taylor & Francis, London (1974).
13. C. N. R. RAO, D. J. BUTTREY, N. OTSUKA, P. GANGULY, H. R. HARRISON, C. J. SANDBERG, AND J. M. HONIG, *J. Solid State Chem.* **51,** 266 (1984).
14. L. N. BULAEVSKII, E. L. NAGAEV, AND D. I. KHOMSKII, *Sov. Phys. JETP* **27,** 836 (1968); E. L. Nagaev, *Sov. Phys. JETP* **31,** 682 (1970).
15. J. E. HIRSCH, *Phys. Rev. Lett.* **59,** 228 (1987).
16. V. J. EMERY, *Phys. Rev. Lett.* **58,** 2794 (1987).
17. M. M. MOHAN AND N. KUMAR, *J. Phys. C* **20,** L527 (1987).
18. N. KUMAR, *Physica C* **153,** 1227 (1988).
19. M. M. MOHAN, *Nucl. Phys. B* **5A,** 145 (1988).
20. M. GURVITCH AND A. T. FIORI, *in* "Novel Mechanisms of Superconductivity" (S. A. Wolf and V. Z. Kresin, Eds.), Plenum, New York (1987).
21. "Studies in High Temperature Superconductivity," Nova Science, New York (1989).
22. WARREN E. PICKETT, *Rev. Mod. Phys.* **61,** 433 (1989).
23. M. CYROT, *J. Phys. Coll. C* **49**(8), 2227 (1989).
24. "Mechanisms of High Temperature Superconductivity" (H. Kamimura and A. Oshiyama, Eds.), Springer-Verlag, Berlin (1989).
25. W. WEBER, Festkörper probleme: "Advances in Solid State Physics" (1989).
26. J. FRIEDEL, *J. Phys. Condens. Matter* **1,** 7757 (1989).
27. For a concise general outlook, see "MRS Bulletin" (1989).
28. ROBERT J. BIRGENEAU AND GEN SHIRANE, *in* "Physical Properties of High Temperature Superconductivity" (D. M. Ginsberg, Ed.), Vol. 1, p. 151, World Scientific, Singapore (1989).
29. SUDIP CHAKRAVARTY, BERTRAND I. HALPERIN, AND DAVID R. NELSON, *Phys. Rev. Lett.* **60,** 1057 (1988).
30. F. MEHRAN AND P. W. ANDERSON, *Solid State Commun.* **71,** 29 (1989).
31. J. T. MARKERT, Y. DALICHAOUCH, AND M. B. MAPLE, *in* "Physical Properties of High Temperature Superconductivity" (D. M. Ginsberg, Ed.), Vol. 1, p. 265, World Scientific, Singapore (1989).
32. K. HASS, *in* "Solid State Physics" (Ehrenreich and D. Turnbull, Eds.), Vol. 42, Academic Press, New York (1989).
33. F. C. ZHANG AND T. M. RICE, *Phys. Rev. B* **37,** 3759 (1988).
34. LAURA M. ROTH, *Phys. Rev. Lett.* **60,** 379 (1988).
35. J. E. HIRSCH, *Phys. Rev. Lett.* **54,** 1317 (1985).
36. W. F. BRINKMAN AND T. M. RICE, *Phys. Rev. B* **2,** 1324 (1970); N. Ohata and R. Kubo, *J. Phys. Soc. (Japan)* **28,** 1402 (1970).
37. N. KUMAR, *Phys. Rev. B* **40,** 844 (1989).
38. E. DAGOTTO *et al.*, NSF-ITP-88-176 (preprint, 1989).
39. E. DAGATTO *et al.*, NSF-ITP-89-74 (preprint, 1989).
40. BORIS I. SHRAIMAN AND ERIC D. SIGGIA, *Phys. Rev. Lett.* **60,** 740 (1988).
41. I. O. KULIK AND A. G. PEDAN, *Sov. Phys. JETP* **52,** 742 (1980); P. Nozieres and S. Schmitt. Rink, *J. Low Temp. Phys.* **59,** 195 (1985).
42. J. E. HIRSCH *et al.*, *Phys. Rev. B* **37,** 243 (1989).
43. ZHAO-BIN-SU AND YU LU, IC/88/427 (ICTP Preprint, 1988).
44. C. M. VARMA, P. B. LITTLEWOOD, AND S. SCHMITT RINK, *Phys. Rev. Lett.* **63,** 1966 (1989).